

Double Auger decay in atoms: Probability and angular distribution

M. Ya. Amusia*

*Institut für Theoretische Physik, Universität Frankfurt am Main,
D-6000 Frankfurt am Main 11, Germany*

I. S. Lee†

Fritz-Haber-Institut der Max-Planck-Gesellschaft, Faradayweg 4-6, D-1000 Berlin 33, Germany

V. A. Kilin

Tomsk Polytechnic Institut, Tomsk 634004, Russia

(Received 15 July 1991)

Within many-body perturbation theory (MBPT), the correlated decay of an inner-shell vacancy, namely, the double Auger effect, is considered. Expressions for the amplitude and probabilities are obtained in the lowest order of MBPT. The approximate formulas, in particular the “shakeoff” model, are discussed. The calculations are performed for the $1s^{-1} \rightarrow 2s^{-2}2p^{-1} + q_1 + q_2$ transition in Ne. It is shown that the angular distribution of electrons ejected in the double Auger decay of an s hole is asymmetric, depending strongly on the angle of their relative motion.

PACS number(s): 32.80.Hd

I. INTRODUCTION

In the normal Auger process, filling of a vacancy in an inner shell by an outer-shell electron leads to the emission of a second outer electron. However, if we have a vacancy in a deep inner shell, the transition of the outer electron can cause ejection of two electrons simultaneously, the so-called double Auger (DA) process, Fig. 1. The DA decay was observed for the first time in [1]. Recently, evidence for the analogous resonant process was reported by Becker *et al.* [2]. Unlike the experiment of Carlson and Krause, here they excited the electron from an inner shell to an unoccupied discrete level. Then this excited state with one excited electron and one core hole decayed via ejection of two electrons.

From the analysis of Carlson and Krause [1], it follows that the portion of the triple ions, Ne^{3+} being produced after the DA decay is 8%. The first attempt to calculate the probability of the DA process has been done by Carlson and Krause [1]. Using the “shake-off” model, they determined that the portion of Ne^{3+} ions produced can only be 0.5%, which of course is small compared to the 8% observed in the experiment. One of the possible reasons for such a discrepancy may be the neglect of the shakeoff model to accurately account for electron correlations in the calculation of the DA decay probability.

In this paper we report calculations of the probability of the DA decay within many-body perturbation theory. We also report our investigation of the angular distribution of electrons ejected in the DA process. Section II contains the general formulas for the amplitude of the DA decay in the many-body perturbation theory (MBPT) [3]. In Sec. III the approximate formulas for the amplitude and the probability of the DA decay are presented. Section IV is devoted to the investigation of the energy distribution between two outgoing electrons. The calcu-

lation of the angular distribution of electrons is discussed in Secs. V and VI. The results of the numerical calculations in Ne are presented in Sec. VII.

II. AMPLITUDE OF DOUBLE AUGER DECAY

In the independent-particle model (the “frozen-core” approximation), the amplitude of the DA decay has to be zero since the initial Ψ_i and the final Ψ_f wave functions differ by more than two single-electron states. In this case, as is well known [4], the matrix element $\langle \Psi_f | \hat{V} = 1/r_{12} | \Psi_i \rangle$, determining the amplitude of the DA decay, is zero. Therefore, for the calculation of the DA probability it is necessary to take the many-electron correlations into account. In our work we employ the many-body perturbation theory [3] for the calculation of the DA amplitude.

The initial state in the DA process has only one hole in its electron configuration, while the final state has three vacancies and two electrons in the continuum. Let the lines with the arrows to the left and to the right denote vacancies and electrons, respectively. In this case in the

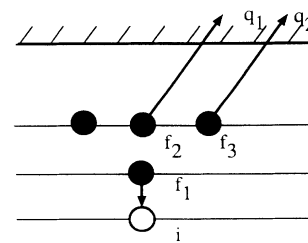


FIG. 1. Schematic representation of the double Auger decay; i is an inner-shell hole.

lowest order of perturbation theory on the interelectron interaction, the amplitude M of the DA decay will be defined by the diagrams shown in Fig. 2. The corresponding analytical expressions are presented as follows:

$$M = \sum_{i=1}^9 M_i, \quad (1)$$

$$\begin{aligned} M_1 &= \sum_k \frac{\langle iq_1 | U | f_1 k \rangle \langle kq_2 | U | f_2 f_3 \rangle}{\varepsilon_i + \varepsilon_{q_1} - \varepsilon_{f_1} - \varepsilon_k}, \\ M_2 &= \sum_k \frac{\langle iq_1 | U | f_2 k \rangle \langle kq_2 | U | f_3 f_1 \rangle}{\varepsilon_i + \varepsilon_{q_1} - \varepsilon_{f_2} - \varepsilon_k}, \\ M_3 &= \sum_k \frac{\langle iq_1 | U | f_3 k \rangle \langle kq_2 | U | f_1 f_2 \rangle}{\varepsilon_i + \varepsilon_{q_1} - \varepsilon_{f_3} - \varepsilon_k}, \\ M_4 &= \sum_k \frac{\langle q_1 q_2 | U | f_1 k \rangle \langle kq_1 | U | f_1 f_2 \rangle}{\varepsilon_{q_1} + \varepsilon_{q_2} - \varepsilon_{f_1} - \varepsilon_k}, \\ M_5 &= \sum_k \frac{\langle q_1 q_2 | U | f_2 k \rangle \langle kq_1 | U | f_3 f_1 \rangle}{\varepsilon_{q_1} + \varepsilon_{q_2} - \varepsilon_{f_2} - \varepsilon_k}, \\ M_6 &= \sum_k \frac{\langle q_1 q_2 | U | f_3 k \rangle \langle kq_1 | U | f_1 f_2 \rangle}{\varepsilon_{q_1} + \varepsilon_{q_2} - \varepsilon_{f_3} - \varepsilon_k}, \\ M_7 &= \sum_k \frac{\langle iq_2 | U | f_1 k \rangle \langle kq_1 | U | f_2 f_3 \rangle}{\varepsilon_i + \varepsilon_{q_2} - \varepsilon_{f_1} - \varepsilon_k}, \\ M_8 &= \sum_k \frac{\langle iq_2 | U | f_2 k \rangle \langle kq_1 | U | f_3 f_1 \rangle}{\varepsilon_i + \varepsilon_{q_2} - \varepsilon_{f_2} - \varepsilon_k}, \\ M_9 &= \sum_k \frac{\langle iq_2 | U | f_3 k \rangle \langle kq_1 | U | f_1 f_2 \rangle}{\varepsilon_i + \varepsilon_{q_2} - \varepsilon_{f_3} - \varepsilon_k}, \end{aligned} \quad (2)$$

where

$$\langle pq | U | rs \rangle = \langle pq | V | rs \rangle - \langle pq | V | sr \rangle \quad (3)$$

is the difference of the ‘‘direct’’ and the ‘‘exchange’’ matrix elements of the Coulomb interaction; i is the initial hole and f_1, f_2, f_3 are the final vacancies; q_1 and q_2 are the Auger electrons; and ε is the one-particle Hartree-Fock energy. The summation over k in (2) implies the summation over the hole and the discrete electron levels and the integration over the continuous spectrum. In the general case, the amplitude M of the DA process has to depend on the total orbital and spin momenta of the initial and final states. The derivation of such an expression is given in the Appendix.

The transition energy in the DA

$$E_{\text{tot}} = E_f - E_i, \quad (4)$$

where E_i and E_f are the energies of the initial and final states, respectively, and is continuously distributed between the two emitted electrons. Therefore, the total probability of the DA process (or its partial width) is determined by the expression

$$\Gamma_i^{\text{DA}} = \int_0^{E_{\text{tot}}} \gamma(E_1) dE_1, \quad (5)$$

where $\gamma(E_1)$ is the probability that the first electron (for

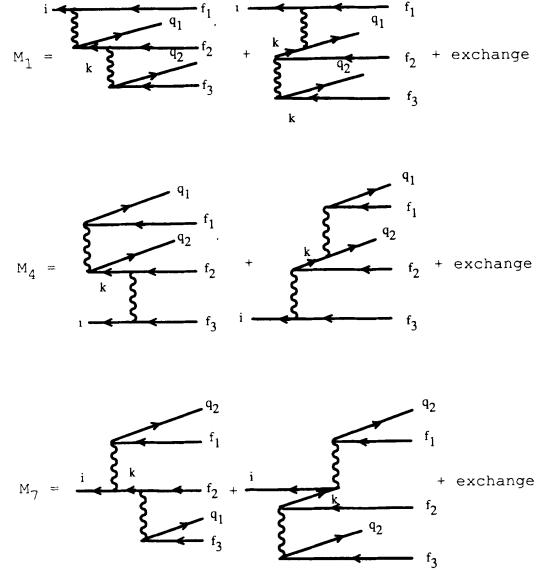


FIG. 2. Brueckner-Goldstone diagrams for the partial amplitudes M_1 , M_4 , and M_7 . Other amplitudes (M_2 and M_3 , M_5 and M_6 , and M_8 and M_9) can be obtained out of amplitudes M_1 , M_4 , and M_7 by the cyclic replacement of the electrons f_1 , f_2 , and f_3 , respectively. Lines with arrows to the left and to the right denote holes and particles, respectively.

example, q_1) has the energy E_1 . The expression for $\gamma(E_1)$ is given [5] by

$$\gamma(E_1) = 2\pi |M|^2. \quad (6)$$

Atomic units are used throughout this paper, while the energy is in rydbergs.

III. FORMULAS DERIVED IN MODEL APPROACHES

In this section we present the approximate formulas for the amplitude M and the probability of the DA decay.

A. Virtual inelastic scattering

Let us assume that in some cases the following conditions are fulfilled:

$$|M_4| \gg |M_i|, \quad i \neq 4 \quad (7a)$$

$$|\text{Im}M_4| \gg |\text{Re}M_4|. \quad (7b)$$

This means that the diagram presented in Fig. 3, namely its imaginary part, dominates in the total amplitude. In this case, the total amplitude of the DA process can be approximately presented as

$$|M| \approx |\text{Im}M_4| \approx \langle k_0 i | U | f_2 f_3 \rangle \langle q_1 q_2 | U | f_1 k_0 \rangle, \quad (8)$$

where $\varepsilon_0 = k_0^2$ satisfies the energy conservation law $\varepsilon_0 = \varepsilon_{f_2} + \varepsilon_{f_3} - \varepsilon_i$. Substituting (8) into expression (6), we find that

$$\Gamma_i^{\text{DA}} \approx \Gamma_{i \rightarrow f_2 f_3 k_0}^A \sigma_{k_0}, \quad (9)$$

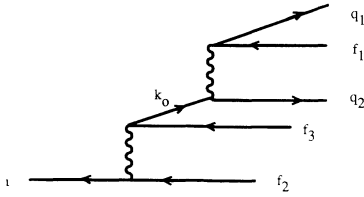


FIG. 3. Diagram describing the inelastic mechanism of the double Auger decay. At the first step the initial vacancy i decays via the normal Auger decay $i^{-1} \rightarrow f_2^{-1} f_3^{-1} + k_0$, the emitted electron k_0 scatters inelastically on the shell f_1 . As the result of such inelastic scattering, two double Auger electrons q_1 and q_2 are ejected.

where $\Gamma_{i \rightarrow f_2 f_3 k_0}^A$ is the probability (width) of the normal Auger decay of the initial hole i and σ_{k_0} is the cross section of the inelastic scattering of the “intermediate” Auger electron k_0 upon the electron shell f_1 . Here the energy distribution of two outgoing electrons is determined by the inelastic scattering process of the k_0 Auger electron and if ϵ_0 is high enough $\epsilon_{q_2} \gg \epsilon_{q_1}$.

B. Cascade mechanism

The initial hole i can decay via the normal Auger transition, producing a vacancy in one of the intermediate shells. This intermediate vacancy, in turn, can decay via another Auger transition.

This mechanism of the DA transition is given symbolically by the diagram shown in Fig. 4. The corresponding probability Γ_i^{DA} is obtained from the expression

$$\Gamma_i^{\text{DA}} \simeq \Gamma_{i \rightarrow f_1 j q_1}^A \Gamma_{j \rightarrow f_2 f_3 q_2}^A \Gamma_j^{-1}, \quad (10)$$

where Γ_j is the total width of the intermediate hole j . The energy spectrum of ϵ_{q_1} and ϵ_{q_2} has two lines centered at $\epsilon_{q_1} = \epsilon_{f_1} + \epsilon_j - \epsilon_i$ and $\epsilon_{q_2} = \epsilon_{f_2} + \epsilon_{f_3} - \epsilon_j$.

C. “Shake-off” model

In this subsection, we will show that MBPT contains the shake-off model as well. In fact, if one restricts oneself in the sum (1) by the terms $M_1|_{k=f_2}$, $M_2|_{k=f_1}$, and $M_9|_{k=i}$, i.e.,

$$M = M_1|_{k=f_2} + M_2|_{k=f_1} + M_9|_{k=i}, \quad (11)$$

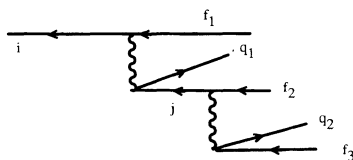


FIG. 4. Auger cascade mechanism of the DA decay. At the first stage the initial hole i decays via the normal $i^{-1} \rightarrow f_2^{-1} j^{-1} + q_1$ Auger process. The intermediate hole j in turn decays via another Auger transition, $j^{-1} \rightarrow f_2^{-1} f_3^{-1} + q_2$.

then

$$\begin{aligned} M &= \langle i q_1 | U | f_1 f_2 \rangle [\langle q_2 i | U | f_3 i \rangle - \langle q_2 f_1 | U | f_3 f_1 \rangle \\ &\quad - \langle q_2 f_2 | U | f_3 f_2 \rangle] (\epsilon_{q_2} - \epsilon_{f_3})^{-1} \\ &\equiv \langle i q_1 | U | f_1 f_2 \rangle (F^{(i)} - F^{(f_1)} - F^{(f_2)}) (\epsilon_{q_2} - \epsilon_{f_3})^{-1}. \end{aligned} \quad (12)$$

In (12), the expression

$$F^{(i)} - F^{(f_1)} - F^{(f_2)} \quad (13)$$

is the alteration of the self-consistent Hartree-Fock field of the atom caused by the normal $i^{-1} \rightarrow f_1^{-1} f_2^{-1} + q_1$ Auger transition. Further, one can easily show, e.g., by applying the perturbation theory in matrix elements in U , that

$$\frac{\langle q_2 | F^{(i)} - F^{(f_1)} - F^{(f_2)} | f_3 \rangle}{\epsilon_{q_1} - \epsilon_{q_3}} \quad (14)$$

is the overlap integral between two one-electron wave functions $\tilde{\varphi}_{f_3}(r)$ and $\tilde{\varphi}_{q_2}(r)$ determined in the field of the initial hole i and in the field of vacancies f_1 and f_2 , respectively [6]. Consequently, the probability of the DA decay will be defined by the equation

$$\Gamma_i^{\text{DA}} = \Gamma_{i \rightarrow f_1 f_2 q_1}^A |\langle \tilde{q}_2 | \tilde{f}_3 \rangle|^2. \quad (15)$$

Here $\langle \tilde{q}_2 |$ and $|\tilde{f}_3 \rangle$ stand for the wave functions $\tilde{\varphi}_{f_3}(r)$ and $\tilde{\varphi}_{q_2}(r)$, respectively. Thus expression (12) corresponds to the shake-off model [1]. In our case the “shaking” of the atomic field is caused by the normal Auger transition $i^{-1} \rightarrow f_1^{-1} f_2^{-1} + q_1$. Finally it should be noted that one can obtain formulas similar to the expression (15) containing other overlap integrals, such as

$$\langle \tilde{q}_2 | \tilde{f}_1 \rangle, \langle \tilde{q}_2 | \tilde{f}_2 \rangle, \langle \tilde{q}_1 | \tilde{f}_1 \rangle, \langle \tilde{q}_1 | \tilde{f}_2 \rangle, \langle \tilde{q}_1 | \tilde{f}_3 \rangle. \quad (16)$$

In this case the energy ϵ_{q_1} and ϵ_{q_2} distribution is strongly asymmetric, having one fast and one slow electron.

IV. ENERGY DISTRIBUTION BETWEEN TWO AUGER ELECTRONS

In the DA process, as mentioned above, the transition energy $E_{\text{tot}} = E_f - E_i$ is continuously distributed between the two outgoing electrons, i.e., each of the electrons may have a kinetic energy between 0 and E_{tot} . We will show below that the most probable situation is the asymmetric partitioning case, where one of the ejected electrons carries away almost the whole energy, while the other electron has only a very small part of it. Therefore in an experiment the observation of a slow and a fast electron would be most probable. It means also, that rather probable is the process with the slow electron captured to a discrete level in the ion state with three vacancies f_1, f_2, f_3 .

Let us start with the case when the energies of both

Auger electrons are relatively high and approximately equal, $\varepsilon_1 \approx \varepsilon_2$. In this case, in order to evaluate the Coulomb matrix elements containing the wave functions $\varphi_{q_1}(r)$ and $\varphi_{q_2}(r)$ of electrons q_1 and q_2 , one may replace $\varphi_{q_1}(r)$ and $\varphi_{q_2}(r)$ by the plane waves $e^{i\kappa_{q_1}r}$ and $e^{i\kappa_{q_2}r}$, respectively; then the Coulomb matrix elements prove to be of the order of $(\kappa_{q_i})^{-\beta}$, where $\kappa_{q_i} = (\varepsilon_{q_i})^{1/2}$, $i = 1, 2$ [7]. The corresponding amplitudes will be of the order of

$$E_{\text{tot}}^{-(\beta+1)} \quad (\beta > 1). \quad (17)$$

The magnitude β depends on the angular momentum transferred via the Coulomb interaction.

Now let us consider another case, when $\varepsilon_{q_1} \approx 0$, $\varepsilon_{q_2} \approx E_{\text{tot}}$. Here we cannot replace the wave function of the slow electron by the plane wave. However, at least for estimation of the Coulomb matrix elements, we can use the Coulombic wave function of the electron having zero energy [8],

$$R_{El}|_{E=0} \sim \sqrt{r} I_{2l+1}(\sqrt{8r}). \quad (18)$$

Here $I_l(r)$ is the Bessel function. Substituting (18) into the Coulomb matrix elements, one obtains

$$M_i \sim E_{\text{tot}}^{-\beta/2}. \quad (19)$$

Comparing (17) and (19) we see that in the second case, when the transition energy is distributed asymmetrically ($\varepsilon_1 \gg \varepsilon_2$), the partial amplitudes and consequently the probability may in principle exceed those of the symmetric distribution ($\varepsilon_1 \approx \varepsilon_2$). These qualitative arguments are corroborated by the numerical calculations given below.

The expressions (17) and (19) also help to explain the behavior of the DA decay probability when passing from the 1s-hole decay in Ne to that of the 3d vacancy in Kr. Carlson and Krause [9] observed that in Kr the yield of the triple ions is 31%, while in Ne it is only 8%. According to the expressions (16) and (18) the amplitude of the DA decay in Kr can be larger than in Ne, since in the

former case the transition energy is smaller. Therefore, if the incidental cancellation of the "partial" amplitudes M_i ($i = 1, 2, \dots, 9$) in the total amplitude $M = \sum_i M_i$ does not take place, then one should expect that in Kr, where the excess energy is much less than in the decay of the 1s hole in Ne, the probability of the DA decay of the 3d hole will be larger than one of the 1s hole decay in Ne.

V. ANGULAR DISTRIBUTION

Within the framework of the statistical tensor formalism [10], the probability W of emitting two electrons in directions \mathbf{n}_1 and \mathbf{n}_2 can be written as

$$\frac{dW}{d\varepsilon_1 d\mathbf{n}_1 d\mathbf{n}_2} = \sum_{\substack{k,q,I_1,I'_1 \\ l_1,j_1,l_2,j_2}} M(l_1 j_1, l_2 j_2) \rho_{kq}(I, I) \\ \times \varepsilon_{kq}(I, I) M^*(l_1 j_1, l_2 j_2), \quad (20)$$

where $\rho_{kq}(I, I)$ is the statistical tensor of the initial state, I is the total angular momentum of the initial ion, $\varepsilon_{kq}(I, I)$ is the efficiency tensor, $M(l_1 j_1, l_2 j_2)$ is the DA amplitude; $l_i j_i$ ($i = 1, 2$) are the orbital and total momenta of the electrons, and ε_1 is the energy of one of the electrons ejected, for example the first one.

The expressions for the amplitude $M(l_1 j_1, l_2 j_2)$ of the DA decay are presented in Sec. II and the Appendix. It is only necessary to take into account that in calculations of the angular distribution we choose the following coupling scheme:

$$\Psi_f = |I_f, (l_1 j_1, l_2 j_2) I_1 : I \rangle, \quad (21)$$

that is, the pair of ejected Auger electrons is characterized by the total momentum I_1 .

Let us consider the efficiency tensor $\varepsilon_{kq}(I, I)$. According to the common rules we can construct $\varepsilon_{kq}(I, I)$ using the tensors $\varepsilon_{k_f q_f}(I_f, I_f)$ of the final ion and the tensor $\varepsilon_{k_0 q_0}(I_1, I_1)$ responsible for the pair of outgoing electrons [10],

$$\varepsilon_{kq}(I, I) = \sum_{k_f, q_f, k_0, q_0} \langle I_f I_1(I) I_f I'_1(I) : k | I_f I_f(k_f) I_1 I'_1(k_0) : k \rangle (k_f q_f k_0 q_0 | k q) \varepsilon_{k_f q_f}(I_f, I_f) \varepsilon_{k_0 q_0}(I_1, I'_1), \quad (22)$$

where

$$\langle I_f I_1(I) I_f I'_1(I) : k | I_f I_f(k_f) I_1 I'_1(k_0) : k \rangle \quad (23)$$

is the recoupling coefficient and $(a\alpha b\beta | c\gamma)$ is the Clebsch-Gordan coefficient. Further, we consider the case when the final ion is not observed. Then the efficiency tensor of the final ion is determined by the equation [10]

$$\varepsilon_{k_f q_f}(I_f I_f) = \delta_{k_f 0} \delta_{q_f 0} \hat{I}_f^{-1}. \quad (24)$$

Here $\hat{I} = (2I + 1)^{1/2}$. In this case

$$\langle I_f I_1(I) I_f I'_1(I) : k | I_f I_f(k_f) I_1 I'_1(k_0) : k \rangle = \hat{I}^{-2} \hat{I}_f^{-1} (-1)^{I+I_f+I'_1+k_0} \begin{Bmatrix} I_1 & I & I_f \\ I & I'_1 & k_0 \end{Bmatrix}. \quad (25)$$

Substituting (24) and (25) into (22) we get

$$\varepsilon_{kq}(I, I) = \hat{I}^2 \hat{I}_f^{-2} (-1)^{I+I_f+I'_1+k} \begin{Bmatrix} I_1 & I & I_f \\ I & I'_1 & k \end{Bmatrix} \varepsilon_{kq}(I_1, I'_1). \quad (26)$$

The tensor $\epsilon_{kq}(I_1, I'_1)$ describing the pair of the Auger electrons, can be constructed from the tensors of individual electrons, that is, from $\epsilon_{k_1 q_1}(j_1, j'_1)$ and $\epsilon_{k_2 q_2}(j_2, j'_2)$, respectively,

$$\epsilon_{kq}(I_1, I'_1) = \sum_{k_1, q_1, k_2, q_2} \hat{I}_1 \hat{I}'_1 \hat{k}_1 \hat{k}_2 \begin{Bmatrix} j_1 & j_2 & I_1 \\ j'_1 & j'_2 & I'_1 \\ k_1 & k_2 & k \end{Bmatrix} (k_1 q_1 k_2 q_2 | k q) \epsilon_{k_1 q_1}(j_1, j'_1) \epsilon_{k_2 q_2}(j_2, j'_2). \quad (27)$$

Finally, we get

$$\begin{aligned} \epsilon_{kq}(I_1, I'_1) &= \frac{1}{16\pi} \hat{I}^2 \hat{I}'^2 \hat{I}_f^{-2} \hat{I}_1 \hat{I}'_1 (-1)^{I+I_f+I'_1+k+1+j'_1+j'_2} \\ &\times \sum_{k_1, q_1, k_2, q_2} \hat{l}_1 \hat{j}_1 \hat{l}'_1 \hat{j}'_1 \hat{l}_2 \hat{j}_2 \hat{l}'_2 \hat{j}'_2 \begin{Bmatrix} I_1 & I'_1 & k \\ I & I & I_f \end{Bmatrix} \begin{Bmatrix} j_1 & j'_1 & k_1 \\ l'_1 & l_1 & \frac{1}{2} \end{Bmatrix} \begin{Bmatrix} j_2 & j'_2 & k_2 \\ l'_2 & l_2 & \frac{1}{2} \end{Bmatrix} \\ &\times (l_1 0 l'_1 0 | k_1 0) (l_2 0 l'_2 0 | k_2 0) \begin{Bmatrix} j_1 & j_2 & I_1 \\ j'_1 & j'_2 & I'_1 \\ k_1 & k_2 & k \end{Bmatrix} \\ &\times (k_1 q_1 k_2 q_2 | k q) Y_{k_1 q_1}(\mathbf{n}_1) Y_{k_2 q_2}(\mathbf{n}_2). \end{aligned} \quad (28)$$

Substituting (28) into (20) we find

$$\begin{aligned} \frac{dW}{d\varepsilon_1 d\mathbf{n}_1 d\mathbf{n}_2} &= \frac{1}{16\pi} \sum_{k, q} \hat{I}^2 \hat{I}'^2 \hat{I}_f^{-2} \hat{I}_1 \hat{I}'_1 (-1)^{I+I_f} (-1)^{I'_1+k+1} \begin{Bmatrix} I_1 & I'_1 & k \\ I & I & I_f \end{Bmatrix} \rho_{kq}(I, I) \\ &\times \sum_{j_1, l'_1, j'_1, l_2, j_2, l'_2, j'_2, k_1, k_2} \hat{l}_1 \hat{j}_1 \hat{l}'_1 \hat{j}'_1 \hat{l}_2 \hat{j}_2 \hat{l}'_2 \hat{j}'_2 (-1)^{j'_1+j'_2} \begin{Bmatrix} j_1 & j'_1 & k_1 \\ l'_1 & l_1 & \frac{1}{2} \end{Bmatrix} \begin{Bmatrix} j_2 & j'_2 & k_2 \\ l'_2 & l_2 & \frac{1}{2} \end{Bmatrix} \\ &\times (l_1 0 l'_1 0 | k_1 0) (l_2 0 l'_2 0 | k_2 0) \begin{Bmatrix} j_1 & j_2 & I_1 \\ j'_1 & j'_2 & I'_1 \\ k_1 & k_2 & k \end{Bmatrix} \\ &\times Y_{kq}^{k_1 k_2}(\mathbf{n}_1, \mathbf{n}_2) M(l_1 j_1, l_2 j_2) M^*(l_1 j_1, l'_2 j'_2), \end{aligned} \quad (29)$$

where

$$Y_{kq}^{k_1 k_2}(\mathbf{n}_1, \mathbf{n}_2) = \sum_{q_1, q_2} (k_1 q_1 k_2 q_2 | k q) Y_{k_1 q_1}(\mathbf{n}_1) Y_{k_2 q_2}(\mathbf{n}_2). \quad (30)$$

The expression (29) defines the angular distribution of electrons ejected in the DA decay of any vacancy.

For the case of the unpolarized holes (the isotropic system) when [10]

$$\rho_{kq} = \delta_{k0} \delta_{q0} \hat{I}^{-1}, \quad (31)$$

the expression (29) is simplified,

$$W(\Theta_{12}) = N \left[1 + \sum_{k>0} a_k(\varepsilon_1, \varepsilon_2) P_k(\cos \Theta_{12}) \right], \quad (32)$$

where $a_k(\varepsilon_1, \varepsilon_2)$ is given by

$$\begin{aligned} a_k(\varepsilon_1, \varepsilon_2) &= N^{-1} \sum_{\substack{l_1, j_1, l'_1, j'_1 \\ l_2, j_2, l'_2, j'_2}} \hat{l}_1 \hat{j}_1 \hat{l}'_1 \hat{j}'_1 \hat{l}_2 \hat{j}_2 \hat{l}'_2 \hat{j}'_2 (-1)^{j_2+j'_2+I_1} (l_1 0 l'_1 0 | k_1 0) (l_2 0 l'_2 0 | k_2 0) \\ &\times \begin{Bmatrix} j_1 & j'_1 & k \\ l'_1 & l_1 & \frac{1}{2} \end{Bmatrix} \begin{Bmatrix} j_2 & j'_2 & k \\ l'_2 & l_2 & \frac{1}{2} \end{Bmatrix} \begin{Bmatrix} j_1 & j_2 & J_1 \\ j'_2 & j'_1 & k \end{Bmatrix} M(l_1 j_1, l_2 j_2) M^*(l_1 j_1, l'_2 j'_2), \\ N &= \sum_{l_1, j_1, l_2, j_2} |M(l_1 j_1, l_2 j_2)|^2, \end{aligned} \quad (33)$$

$P_k(\cos\Theta_{12})$ is the Legendre polynomial, and Θ_{12} is the angle between directions \mathbf{n}_1 and \mathbf{n}_2 .

Thus the angular distribution of electrons emitted in the double Auger decay of unpolarized vacancies, for example s holes, depends, as it should only on the angle between the two outgoing electrons. In this case, it is expedient to introduce the angular correlation function $F(\Theta_{12})$ [10],

$$F(\Theta_{12}) = 1 + \sum_{k>0} a_k(\epsilon_1, \epsilon_2) P_k(\cos\Theta_{12}), \quad (34)$$

which is normalized in the following way:

$$\frac{1}{16\pi^2} \int F(\Theta_{12}) d\Omega_1 d\Omega_2 = 1. \quad (35)$$

VI. $LS(J)$ APPROXIMATION

Very often it is supposed that the initial and the final states in Auger processes can be characterized by quantum numbers L , S , and J (see, for example [11]). The purpose of this section is the derivation of the formulas in the $LS(J)$ coupling scheme. The transformation of the amplitude of the DA decay into the LS representation is carried out, as well as for the normal Auger process according to the known expression [11]. In our case, we get

$$\begin{aligned} M(l_1 j_1, l_2 j_2) &= \hat{I}_f \hat{I}_1 \hat{L}_1 \hat{S}_1 \hat{L} \hat{S} \hat{J}_1 \hat{J}_2 \\ &\times \begin{Bmatrix} l_1 & \frac{1}{2} & j_1 \\ l_2 & \frac{1}{2} & j_2 \\ L_1 & S_1 & J_1 \end{Bmatrix} \begin{Bmatrix} L_f & S_f & I_f \\ L_1 & S_1 & I_1 \\ L & S & J \end{Bmatrix} \\ &\times M(L_f S_f, (l_1 l_2) L_1 S_1). \end{aligned} \quad (36)$$

The amplitudes $M(L_f S_f, (l_1 l_2) L_1 S_1)$ will not depend on the momenta j_1 and j_2 if we neglect by the spin-orbital interaction among Auger electrons. Then substituting (36) into (33) we can perform the summation over j_1, j_1', j_2 , and j_2' ,

$$\begin{aligned} a_k(\epsilon_1, \epsilon_2) &= N^{-1} \sum_{l, l'} (-1)^{k+L_1} \hat{I}_1 \hat{I}_2 \hat{I}'_1 \hat{I}'_2 (l_1 0 l'_1 0 | k 0) \\ &\times (l_2 0 l'_2 0 | k 0) \begin{Bmatrix} l_1 & l_2 & L_1 \\ l'_2 & l'_1 & k \end{Bmatrix} \\ &\times \hat{I}_f^2 \hat{I}_1^2 \hat{L}^2 \hat{S}^2 \begin{Bmatrix} L_f & S_f & I_f \\ L_1 & S_1 & I_1 \\ L & S & J \end{Bmatrix}^2 \\ &\times M(L_1 S_1, l_1 l_2) M(L_1 S_1, l'_1 l'_2), \end{aligned} \quad (37)$$

$$N = \sum_{l_1, l_2} \hat{I}_f^2 \hat{I}_1^2 \hat{L}^2 \hat{S}^2 \begin{Bmatrix} L_f & S_f & I_f \\ L_1 & S_1 & I_1 \\ L & S & J \end{Bmatrix} |M(L_1 S_1, l_1 l_2)|^2. \quad (38)$$

Finally, let us consider the case when both in the final ion and in the continuum, we can neglect the fine structure. We may then perform the summation over I_f and I_1 . In this case $a_k(\epsilon_1, \epsilon_2)$ is defined by the expression

$$\begin{aligned} a_k(\epsilon_1, \epsilon_2) &= (N')^{-1} \sum_{l_1, l_2, l'_1, l'_2} (-1)^{k+L_1} \hat{I}_1 \hat{I}_2 \hat{I}'_1 \hat{I}'_2 (l_1 0 l'_1 0 | k 0) (l_2 0 l'_2 0 | k 0) \\ &\times M(L_1 S_1, l_1 l_2) M^*(L_1 S_1, l'_1 l'_2), \quad N' = \sum_{l_1, l_2} |M(L_1 S_1, l_1 l_2)|^2. \end{aligned} \quad (39)$$

VII. RESULTS OF CONCRETE CALCULATIONS AND DISCUSSION

A. Decay probability

We have calculated the probability for the $1s^{-1}(^2S) \rightarrow 2s^{-2}(^1S) 2p^{-1}(^2P) + q_1 + q_2$ transition in Ne. For the calculations of the Coulomb matrix elements, the Hartree-Fock wave functions were employed. The wave functions of the Auger electrons were defined in the field of the three holes ($2s^{-2} 2p^{-1}$). That allows us to take into account some many-electron correlations [6].

In the DA, the selection rules permit the emission of electrons with the following momenta: $l_{q_1} = 0$, $l_{q_2} = 1$, then $l_{q_1} = 1$, $l_{q_2} = 2$, and so on. However, the calculations show that with increasing values of orbital momenta the contribution of such pairs of electrons is rapidly reduced. For example, in the case under investigation, the contri-

bution of the electron pair with $l_{q_1} = 2$, $l_{q_2} = 3$ is negligible. Therefore we limited ourselves by the calculation of the channel $l_{q_1} = 0$, $l_{q_2} = 1$. The probability of the other channel $l_{q_1} = 1$, $l_{q_2} = 2$ has been estimated using the "shake-off" formula (15). The excess energy in the transition considered is 50.512 Ry. The same values of the "partial" amplitudes M_i are presented in Tables I and II. The behavior of $\gamma(E_1)$ is presented in Fig. 5. The curve is symmetric since both electrons q_1 and q_2 can have the same energy and orbital momenta. The calculations show that the DA process is favored if one of the electrons is slow (low energy) and the other electron is fast (high energy), in accordance with the estimations presented above.

From Tables I and II one can see that the imaginary part [$\text{Im}(M_i)$] in the asymmetric distribution is less than the real part [$\text{Re}(M_i)$]. Here the main contribution to

TABLE I. The partial (M_i , $i=1,2,\dots,9$) and the total M amplitudes (in units of 10^3) for the transition $1s^{-1}\rightarrow 2s^{-2}2p^{-1}(^2P)q_1s(^1P)q_2p(^2S)$ in Ne. E_1 is the energy of the “first” Auger electron in rydbergs. The total energy of the given transition is 50.512 Ry.

	$E_1=0.010$	$E_1=1.000$	$E_1=25.256$	$E_1=49.512$	$E_1=50.502$
M_1	-0.540	-0.413	-0.020	0.468	0.857
M_2	-0.540	-0.413	-0.020	0.468	0.857
M_3	-0.0005	-0.000	-0.005	0.015	0.033
M_4	-0.008 + $i0.083$	-0.004 + $i0.065$	-0.008 + $i0.024$	-0.003 + $i0.017$	-0.005 + $i0.019$
M_5	-0.010 + $i0.079$	-0.006 + $i0.063$	-0.010 + $i0.025$	-0.006 + $i0.020$	-0.007 + $i0.022$
M_6	0.003 + $i0.0075$	-0.013 + $i0.020$	-0.029 + $i0.025$	-0.019 + $i0.105$	-0.025 + $i0.206$
M_7	0.140	0.115	0.013	0.001	0.0005
M_8	0.140	0.115	0.013	0.001	0.0005
M_9	0.362	0.279	-0.107	-1.469	-2.656
M	-0.458 + $i0.169$	-0.344 + $i0.148$	-0.172 + $i0.074$	-0.545 + $i0.142$	-0.947 + $i0.247$
$\gamma_1(E_1)$ (units of 10^6)	1.441	0.837	0.220	1.988	6.060

the total amplitude is given by the shake-off mechanism. The “shaking” of the slow electron is more probable than that of the fast electron since the overlap integral between the outgoing electron and the core electron decreases very rapidly with increasing electron energy (16). Thus, the fast electron is ejected in the “virtual” Auger decay, while the slow electron results in the shake-off process.

If we sum up the probabilities of the transitions $1s^{-1}(^2S)\rightarrow 2s^{-2}(^1S)2p^{-1}(^2P)q_1s(^1P)q_2p(^2S)$ and $1s^{-1}(^2S)\rightarrow 2s^{-2}(^1S)2p^{-1}(^2P)q_1s(^3P)q_2p(^2S)$, then we get the value 0.34×10^{-2} eV or 1.5% of the total width (0.23 eV) of the $1s$ hole [12]. It should be noted that the result of the shakeoff calculations according to expression (15) will be three times less. This implies that it is necessary to take into account all mechanisms in the DA process.

There are also the transitions with the other electron

configuration in the final state to consider, namely the $1s^{-1}\rightarrow 2s^{-2}2p^{-1}+q_1+q_2$ and $1s^{-1}\rightarrow 2p^{-3}+q_1+q_2$ transitions. In these transitions the excess energy will not differ considerably from the first case. Therefore we may assume, in accordance with expressions (17) and (19), that the total probability of these two transitions can be equal to $(0.5-0.6)\times 10^{-2}$ eV. Then the total “double Auger” width of the $1s$ hole will be $\sim 0.9\times 10^{-2}$ eV or 4.0% of the total width of the $1s$ vacancy. This value agrees reasonably well with the experimental result of Carlson and Krause [1]; however, for a more detailed comparison, more comprehensive calculations are necessary.

B. Angular distribution

Numerical calculations have also been carried out for the $1s^{-1}\rightarrow 2s^{-2}2p^{-1}+\varepsilon_1+\varepsilon_2$ transition in Ne. Here also the Auger spectrum can be described in the $LS(J)$ ap-

TABLE II. The partial (M_i , $i=1,2,\dots,9$) and the total M amplitudes (in units of 10^3) for the transition $1s^{-1}\rightarrow 2s^{-2}2p^{-1}(^2P)q_1s(^3P)q_2p(^2S)$ in Ne. Notation is the same as in Table I.

	$E_1=0.010$	$E_1=1.000$	$E_1=25.256$	$E_1=49.512$	$E_1=50.502$
M_1	-0.332	-0.242	-0.005	0.900	1.052
M_2	-0.332	-0.242	-0.005	0.900	1.052
M_3	-0.025	-0.024	-0.006	0.138	0.146
M_4	-0.044 + $i0.035$	-0.018 + $i0.010$	-0.056 + $i0.007$	-0.044 + $i0.003$	-0.041 + $i0.007$
M_5	-0.047 + $i0.036$	-0.017 + $i0.010$	-0.061 + $i0.008$	-0.047 + $i0.006$	-0.044 + $i0.006$
M_6	-0.007 + $i0.023$	-0.035 + $i0.049$	-0.037 + $i0.054$	-0.028 + $i0.280$	-0.032 + $i0.377$
M_7	0.042	0.040	0.019	0.023	0.022
M_8	0.043	0.040	0.019	0.023	0.022
M_9	0.210	+0.133	-0.070	-2.728	-3.264
M	-0.491 + $i0.093$	-0.0365 + $i0.068$	-0.200 + $i0.069$	-0.861 + $i0.289$	-1.087 + $i0.390$
$\gamma_1(E_1)$ (units of 10^6)	1.569	0.864	0.283	5.176	8.371

TABLE III. Contributions of electron pairs with different orbital momenta [$l_1=0$, $l_2=1$ is the (s,p) channel, and so on]; W is the total probability (i) “shake-off” results obtained using the diagrams of Fig. 7, and (ii) MBPT data.

(l_1, l_2)	$\varepsilon_1 \gg \varepsilon_2$		$\varepsilon_1 = \varepsilon_2$
	Shake off	MBPT	MBPT
(s,p)	0.80	0.51	0.72
(p,d)	0.20	0.47	0.22
(d,f)	0.00	0.02	0.06
$W(\varepsilon_1, \varepsilon_2)$	2.13	2.36	0.15

(units of 10^{-5})

proximation, since the spin-orbital interaction is small, and besides the $1s$ hole is unpolarized. Hence, we can employ expression (39) for the description of the angular distribution of the electrons emitted in the DA decay.

We have considered only the following two cases: (i) $\varepsilon_1 \gg \varepsilon_2$, namely, $\varepsilon_1=49.512$ Ry and $\varepsilon_2=1$ Ry, and (ii) $\varepsilon_1=\varepsilon_2=25.256$ Ry. The results of calculations are presented in Tables III and IV. In Table III, total probabilities (integrated over Θ_{12}) are given. One can see that the contribution of the (d,f) pair is negligible. Therefore, to obtain good results, we can only take into account the (s,p) and (d,p) pairs.

The angular distribution coefficients $a_k(\varepsilon_1, \varepsilon_2)$ are given in Table IV. For the case $\varepsilon_1 \gg \varepsilon_2$ we have investigated the influence of the (d,f) pair on the angular distribution.

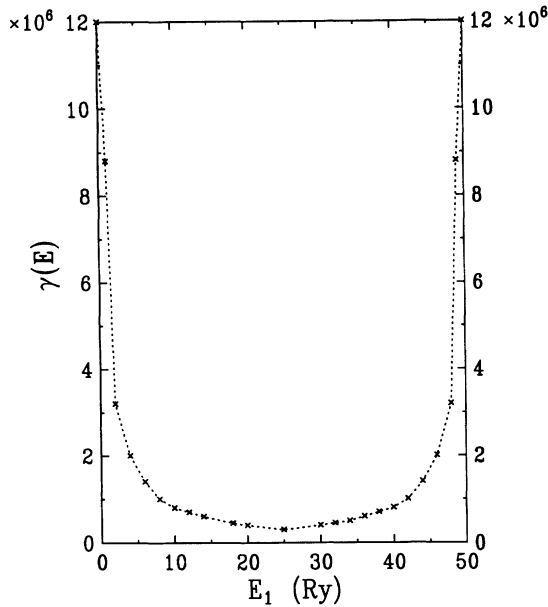


FIG. 5. Dependence of the probability of the DA decay on the distribution of the total energy E_{tot} between two outgoing electrons, the transition $1s^{-1} \rightarrow 2s^{-2}2p^{-1} + q_1 + q_2(^2S)$. The curve is symmetrical as we have taken into account that both electrons q_1 and q_2 may have the same energy and orbital momenta.

TABLE IV. The angular distribution parameters $a_k(\varepsilon_1, \varepsilon_2)$: The shake-off results using the diagrams of Fig. 7, MBPT data, and MBPT results without (d,f) channel.

k	$\varepsilon_1 \gg \varepsilon_2$			$\varepsilon_1 = \varepsilon_2$	
	Shake off	MBPT	MBPT ^a	MBPT	MBPT ^a
1	0.72	0.35	0.52	-1.67	-1.57
2	0.05	0.18	0.21	1.16	0.76
3	0.00	0.29	0.28	-0.39	-0.03
4	0.00	0.05	0.00	0.08	0.00
5	0.00	0.01	0.00	0.02	0.00

^aWithout the (d,f) channel.

This contribution proved to be small and we can neglect it. In Fig. 6 the function $F(\Theta)$ is presented. One can see that there is a dependence of the angle correlation function $F(\Theta)$ on the partitioning of the total energy E between two outgoing electrons. In the first case ($\varepsilon_1 \gg \varepsilon_2$), $F(\Theta)$ decreases with increasing angle Θ_{12} . In contrast, in the second case ($\varepsilon_1 = \varepsilon_2$), we observe a corresponding increase.

It is interesting to compare the MBPT and shake-off results. In Fig. 7 the diagrams that are responsible for the shake-off mechanism in the $1s^{-1} \rightarrow 2s^{-2}2p^{-1} + \varepsilon_1 + \varepsilon_2$ case are presented. One can see that the total probability (after the integration over Θ_{12}) is close to the MBPT result ($\sim 90\%$), while the angular distribution differs considerably.

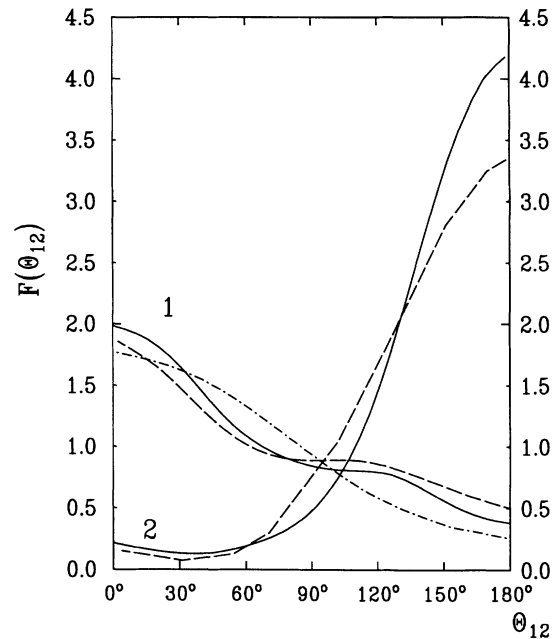


FIG. 6. Angle correlation function $F(\Theta_{12})$: The solid curves 1 and 2 correspond to the cases $\varepsilon_1 \gg \varepsilon_2$ and $\varepsilon_1 = \varepsilon_2$, respectively; the dashed curves represent the same results where, however, the $l_{q_1}=2$, $l_{q_2}=3$ channel is not taken into account; the dash-dotted curve represents the “shake-off” result.

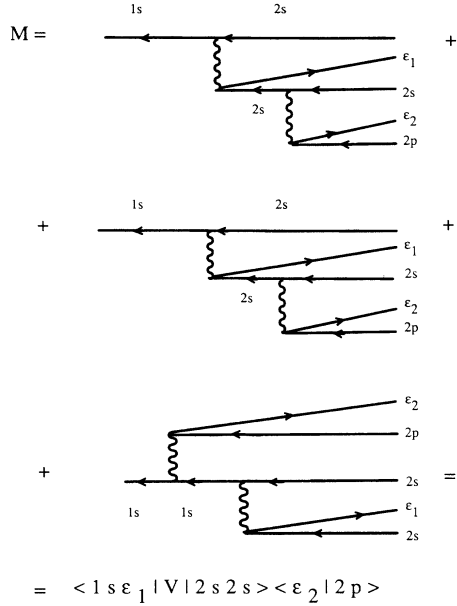


FIG. 7. Diagrams illustrate “shake-off” contribution to the total amplitude for the $1s^{-1} \rightarrow 2s^{-2}2p^{-1} + q_1 + q_2$ case.

VIII. CONCLUSION

Employing the MBPT, we have obtained expressions for the amplitude of the DA decay of an inner-shell vacancy. The relationship between many-body theory and other theoretical approaches is shown. The obtained formulas are useful for the estimation of the DA probabilities in molecules and solid states. According to our qualitative arguments, two features of the behavior of the DA decay are revealed. First, the asymmetric distribution of the total energy between two outgoing electrons is more probable than the symmetric one. Hence in the experiment, slow and fast electrons will mainly be observed. Second, in passing from the decay of the $1s$ hole in Ne to the $2p$ vacancy in Ar and finally to the $3d$ hole in Kr, the probabilities and consequently, the portion of the triple

$$\Psi_f = [[[[\tilde{a}_{f_1} \times \tilde{a}_{f_2}]_{M_{L_1} S_1}^{L_1 S_1} \times \tilde{a}_{f_3}]_{M_{L_2} S_2}^{L_2 S_2} \times \hat{a}_{q_1}^\dagger]_{M_{L_3} S_3}^{L_3 S_3} \times \hat{a}_{q_2}^\dagger]_{M_L S}^{L S} \times |\Phi_0\rangle, \quad (\text{A2})$$

where the state $|\Phi_0\rangle$ has neither holes nor electrons—the “vacuum” state, and $[\hat{a}_i \times \hat{a}_j]_{MM'}^{LS}$ denotes the double-tensor operator product. The difference of the “direct” ($\langle ij | V | pq \rangle$) and “exchange” ($\langle ij | V | qp \rangle$) Coulomb matrix elements can be presented as [6]

$$\langle ij | V | qp \rangle = \sum_{l,m} (-1)^{m_i + m_j + m} \begin{Bmatrix} l_i & l & l_p \\ -m_i & -m & m_p \end{Bmatrix} \times \begin{Bmatrix} l_j & l & l_q \\ -m_j & m & m_q \end{Bmatrix} \times (V_{ijpq}^{(l)} \sigma_{\mu_i \mu_j} \sigma_{\mu_p \mu_q} - W_{ijpq}^{(l)} \sigma_{\mu_i \mu_q} \sigma_{\mu_j \mu_p}), \quad (\text{A3})$$

ions, will increase.

We have also investigated the angular distribution of the electrons ejected in the DA decay. The simplest case has been considered, namely, the decay of the s holes. In this case, the following were proved:

(i) Unlike the normal Auger decay of s vacancies in atoms, the DA of unpolarized holes leads to an asymmetric distribution of the emitted electrons.

(ii) The angular distribution is more sensitive to the approximation used in the calculation of the amplitudes than is the total probability.

ACKNOWLEDGMENTS

The authors thank Professor U. Becker for many helpful discussions. One of the authors (M.A.) is grateful to the Alexander von Humboldt Foundation which has made possible his stay and research in Germany. The other author (I.L.) acknowledges the hospitality of the Fritz-Haber-Institut, where part of this work was performed.

APPENDIX

Here we present the calculation of the spin and the angular parts of the partial amplitudes M_i for the DA process. Let us recall that the operators of creation $\hat{a}_i^\dagger = \hat{a}_{n_i l_i s_i m_i \mu_i}$ and annihilation $\hat{a}_i = \hat{a}_{n_i l_i s_i m_i \mu_i}$ of electrons are the double spherical tensors of rank l_i (with respect to the orbital momentum l_i) and rank s_i (with respect to the spin) [13]. For the creation (\hat{a}_j) and annihilation (\hat{a}_j^\dagger) operators of holes it is necessary to introduce the so-called modified operators \tilde{a}_i defined as

$$\tilde{a}_i \equiv \tilde{a}_{n_i l_i s_i m_i \mu_i} = (-1)^{l_i + s_i - m_i - \mu_i} \hat{a}_{n_i l_i s_i - m_i - \mu_i}. \quad (\text{A1})$$

These are double spherical tensors as well. Using this fact, we can construct the wave functions Ψ_f for the final states in the DA process. The final state has three holes f_1, f_2, f_3 in the core and two electrons q_1, q_2 in the continuum. According to the rules of tensor algebra [13,14] Ψ_f can be written as

where

$$V_{ijpq}^{(l)} = \hat{l}_i \hat{l}_q \hat{l}_p \hat{l}_q \begin{Bmatrix} l_i & l & l_p \\ 0 & 0 & 0 \end{Bmatrix} \begin{Bmatrix} l_j & l & l_q \\ 0 & 0 & 0 \end{Bmatrix} \times \int_0^\infty dr_1 dr_2 P_i(r) P_j(r') \frac{r_{<}^{(l)}}{r_{>}^{(l+1)}} P_p(r) P_q(r') \quad (\text{A4})$$

is the direct and

$$W_{ijpq}^{(l)} = \hat{l}^2 \sum_{l'} (-1)^{l+l'} \begin{Bmatrix} l_i & l & l_p \\ l_j & l' & l_q \end{Bmatrix} V_{ijpq}^{(l')} \quad (\text{A5})$$

is the exchange reduced matrix elements, respectively.

Here $\hat{L} = (2L + 1)^{1/2}$ and the curly brackets enclosing the six terms denote the 6j Wigner symbol, $\begin{pmatrix} abc \\ 000 \end{pmatrix}$ is the 3j coefficient, and $P_i(r)$ is the radial part of the wave functions.

Let us substitute the expressions (A1)–(A5) into the “partial” amplitudes M_i ($i = 1, 2, \dots, 9$). After the summation over the projections $m_i, m_{f_1}, m_{f_2}, m_{f_3}, m_{q_1}, m_{q_1}, m_{q_2}, m_k$, and $\mu_i, \mu_{f_1}, \mu_{f_2}, \mu_{f_3}, \mu_{q_1}, \mu_{q_1}, \mu_{q_2}, \mu_k$ we obtain

$$\begin{aligned}
 M_1 = & \sum_{\substack{n_k, l_k, l_1, l_2 \\ x, y}} (-1)^{L+L_2+l_{f_2}+l_k+l_{q_1}+l_2+y} \hat{L}_1 \hat{L}_2 \hat{L}_3 \hat{L}^{-1} \hat{x}^2 \hat{y}^2 \\
 & \times \begin{Bmatrix} L & l_{f_2} & x \\ L_1 & l_1 & l_{f_1} \end{Bmatrix} \begin{Bmatrix} x & l_k & y \\ l_{q_1} & L_1 & l_1 \end{Bmatrix} \begin{Bmatrix} y & l_{f_3} & L_3 \\ L_2 & l_{q_1} & l_1 \end{Bmatrix} \begin{Bmatrix} L & l_2 & y \\ l_{f_3} & L_3 & l_q \end{Bmatrix} \begin{Bmatrix} L & l_2 & y \\ l_k & x & l_{f_2} \end{Bmatrix} \\
 & \times [AV_{kq_2f_2f_3}^{(l_2)} V_{iq_1f_1k}^{(l_1)} + (-1)^{-S_1} AV_{kq_2f_2f_3}^{(l_2)} W_{iq_1f_1k}^{(l_1)} + (-1)^{-S_1} BW_{kq_2f_2f_3}^{(l_2)} V_{iq_1f_1k}^{(l_1)} \\
 & + (-1)^{-S_1} CW_{kq_2f_2f_3}^{(l_2)} W_{iq_1f_1k}^{(l_1)}] E_{kq_2f_2f_3}^{-1}, \\
 M_2 = & \sum_{\substack{n_k, l_k, l_1, l_2 \\ x, y}} (-1)^{l_{f_1}+l_{f_2}+l_{f_3}+l_k+l_1+l_2} \hat{L}_1 \hat{L}_2 \hat{L}_3 \hat{L}^{-1} \hat{x}^2 \hat{y}^2 \\
 & \times \begin{Bmatrix} L & l_{f_1} & x \\ L_1 & l_1 & l_{f_2} \end{Bmatrix} \begin{Bmatrix} x & l_{q_1} & y \\ l_k & L_1 & l_1 \end{Bmatrix} \begin{Bmatrix} y & L_2 & l_2 \\ l_{f_3} & l_k & L_1 \end{Bmatrix} \begin{Bmatrix} x & l_2 & L_3 \\ L_2 & l_{q_1} & y \end{Bmatrix} \begin{Bmatrix} L & l_{f_1} & x \\ l_2 & L_3 & l_q \end{Bmatrix} \\
 & \times [BV_{kq_2f_3f_1}^{(l_2)} V_{iq_1f_2k}^{(l_1)} - CV_{kq_2f_3f_1}^{(l_2)} W_{iq_1f_2k}^{(l_1)} + (-1)^{-S_1} AW_{kq_2f_3f_1}^{(l_2)} V_{iq_1f_2k}^{(l_1)} + AW_{kq_2f_3f_1}^{(l_2)} W_{iq_1f_2k}^{(l_1)}] E_{kq_2f_3f_1}^{-1}, \\
 M_3 = & \sum_{\substack{n_k, l_k, l_1, l_2 \\ x, y}} (-1)^{L_1+l_{f_3}+l_{q_1}+l_2} \hat{L}_1 \hat{L}_2 \hat{L}_3 \hat{L}^{-1} \begin{Bmatrix} l_k & L_1 & l_{q_2} \\ l_{f_2} & l_2 & l_{f_1} \end{Bmatrix} \begin{Bmatrix} L & l_{f_3} & l_1 \\ L_3 & L_2 & l_{q_1} \\ l_{q_2} & L_1 & l_k \end{Bmatrix} \\
 & \times [(-1)^{+1-S_1} CV_{kq_2f_1f_2}^{(l_2)} V_{iq_1f_3k}^{(l_1)} + (-1)^{-S_1} BV_{kq_2f_1f_2}^{(l_2)} W_{iq_1f_3k}^{(l_1)} - CW_{kq_2f_1f_2}^{(l_2)} V_{iq_1f_3k}^{(l_1)} \\
 & + BW_{kq_2f_1f_2}^{(l_2)} W_{iq_1f_3k}^{(l_1)}] E_{kq_2f_1f_2}^{-1}, \\
 M_4 = & \sum_{\substack{n_k, l_k, l_1, l_2 \\ x, y}} (-1)^{L+L_2+l_{q_1}+l_1+x+y} \hat{L}_1 \hat{L}_2 \hat{L}_3 \hat{L}^{-1} \hat{x}^2 \hat{y}^2 \\
 & \times \begin{Bmatrix} L & x & l_k \\ l_{f_2} & l_2 & l_{f_3} \end{Bmatrix} \begin{Bmatrix} l_{f_1} & y & l_k \\ l_{q_2} & l_1 & l_{q_1} \end{Bmatrix} \begin{Bmatrix} L_2 & y & L \\ l_{q_2} & L_3 & l_{q_1} \end{Bmatrix} \begin{Bmatrix} x & l_k & L \\ y & L_2 & l_{f_1} \end{Bmatrix} \begin{Bmatrix} L_2 & x & l_{f_1} \\ l_{f_2} & L_1 & l_{f_3} \end{Bmatrix} \\
 & \times [(-1)^{1-S_1} CV_{kif_2f_3}^{(l_2)} V_{q_1q_2f_1k}^{(l_1)} - CV_{kif_2f_3}^{(l_2)} W_{q_1q_2f_1k}^{(l_1)} + (-1)^{-S_1} AW_{kif_2f_3}^{(l_2)} V_{q_1q_2f_1k}^{(l_1)} \\
 & + BW_{kif_2f_3}^{(l_2)} W_{q_1q_2f_1k}^{(l_1)}] E_{kif_2f_3}^{-1}, \\
 M_5 = & \sum_{\substack{n_k, l_k, l_1, l_2 \\ x, y}} (-1)^{L+L_2+L_3+l_{f_2}+l_{q_1}+l_1+l_2} \hat{L}_1 \hat{L}_2 \hat{L}_3 \hat{L}^{-1} \hat{x}^2 \hat{y}^2 \\
 & \times \begin{Bmatrix} l_{f_1} & y & l_k \\ l_{q_2} & l_1 & x \end{Bmatrix} \begin{Bmatrix} l_{f_3} & y & L \\ l_{q_2} & L_3 & x \end{Bmatrix} \begin{Bmatrix} l_{f_1} & L_1 & l_{f_2} \\ l_{q_1} & l_1 & x \end{Bmatrix} \begin{Bmatrix} L_3 & l_{q_1} & L_2 \\ L_1 & l_{f_3} & x \end{Bmatrix} \begin{Bmatrix} l_{f_1} & l_2 & L \\ l_{f_3} & y & l_k \end{Bmatrix} \\
 & \times [AV_{kif_3f_1}^{(l_2)} V_{q_1q_2f_2k}^{(l_1)} + (-1)^{-S_1} BV_{kif_3f_1}^{(l_2)} W_{q_1q_2f_2k}^{(l_1)} - CW_{kif_3f_1}^{(l_2)} V_{q_1q_2f_2k}^{(l_1)} \\
 & + (-1)^{1-S_1} W_{kif_3f_1}^{(l_2)} W_{q_1q_2f_2k}^{(l_1)}] E_{kif_3f_1}^{-1},
 \end{aligned}$$

$$\begin{aligned}
M_6 = & \sum_{\substack{n_k, l_k, l_1, l_2 \\ x, y}} (-1)^{L+l_k+l_{q_1}+l_{f_1}} \hat{L}_1 \hat{L}_2 \hat{L}_3 \hat{L}^{-1} \begin{Bmatrix} L_1 & l_1 & L_3 \\ l_{q_1} & L_3 & l_{f_3} \end{Bmatrix} \begin{Bmatrix} L & l_k & L_1 \\ l_1 & L_3 & l_{q_2} \end{Bmatrix} \begin{Bmatrix} L & l_k & L_1 \\ l_{f_1} & l_{f_2} & l_2 \end{Bmatrix} \\
& \times [B\mathcal{V}_{kif_1f_2}^{(l_2)} V_{q_1q_2f_3k}^{(l_1)} + (-1)^{-S_1} A\mathcal{V}_{kif_1f_2}^{(l_2)} W_{q_1q_2f_3k}^{(l_1)} + (-1)^{-S_1} B\mathcal{W}_{kif_1f_2}^{(l_2)} V_{q_1q_2f_3k}^{(l_1)} \\
& + A\mathcal{W}_{kif_1f_2}^{(l_2)} W_{q_1q_2f_3k}^{(l_1)}] E_{kif_1f_2}^{-1}, \\
M_7 = & \sum_{\substack{n_k, l_k, l_1, l_2 \\ x, y}} (-1)^{L_1+L_2+L_3+l_{f_1}+l_{f_3}+l_1+l_2+l_{q_2}+y} \hat{L}_1 \hat{L}_2 \hat{L}_3 \hat{L}^{-1} \hat{x}^2 \hat{y}^2 \\
& \times \begin{Bmatrix} L & y & l_{q_1} \\ l_{f_3} & l_2 & x \end{Bmatrix} \begin{Bmatrix} l_{q_2} & y & L_2 \\ l_{f_3} & L_1 & x \end{Bmatrix} \begin{Bmatrix} L & l_1 & l_k \\ l_{f_2} & l_2 & x \end{Bmatrix} \begin{Bmatrix} L_1 & l_{f_2} & l_{f_1} \\ l_1 & l_{q_2} & x \end{Bmatrix} \begin{Bmatrix} l_{q_1} & y & L \\ l_{q_2} & L_3 & L_2 \end{Bmatrix} \\
& \times [B\mathcal{V}_{kq_1f_2f_3}^{(l_2)} V_{iq_2f_1k}^{(l_1)} + (-1)^{-S_1} B\mathcal{V}_{kq_1f_2f_3}^{(l_2)} W_{q_2if_1k}^{(l_1)} - C\mathcal{W}_{kq_1f_2f_3}^{(l_2)} V_{q_2if_1k}^{(l_1)} + A\mathcal{W}_{kq_1f_2f_3}^{(l_2)} W_{q_2if_1k}^{(l_1)}] E_{kq_1f_2f_3}^{-1}, \\
M_8 = & \sum_{\substack{n_k, l_k, l_1, l_2 \\ x, y}} (-1)^{L+l_k+l_1+l_2+y} \hat{L}_1 \hat{L}_2 \hat{L}_3 \hat{L}^{-1} \hat{x}^2 \hat{y}^2 \\
& \times \begin{Bmatrix} L_1 & l_1 & x \\ l_{q_2} & l_{f_1} & l_{f_2} \end{Bmatrix} \begin{Bmatrix} x & l_2 & y \\ l_{q_1} & l_{q_2} & l_{f_1} \end{Bmatrix} \begin{Bmatrix} y & L & L_2 \\ L_3 & l_{q_1} & l_{q_2} \end{Bmatrix} \begin{Bmatrix} L & l_1 & l_k \\ y & x & l_2 \\ L_2 & L_1 & l_{f_3} \end{Bmatrix} \\
& \times [(-1)^{1-S_1} C\mathcal{V}_{kq_1f_3f_1}^{(l_2)} V_{iq_2f_3k}^{(l_1)} + (-1)^{-S_1} A\mathcal{V}_{kq_1f_3f_1}^{(l_2)} W_{q_2if_2k}^{(l_1)} \\
& + (-1)^{-S_1} B\mathcal{W}_{kq_1f_3f_1}^{(l_2)} V_{q_2if_2k}^{(l_1)} + B\mathcal{W}_{kq_1f_3f_1}^{(l_2)} W_{q_2if_2k}^{(l_1)}] E_{kq_1f_3f_1}^{-1}, \\
M_9 = & \sum_{\substack{n_k, l_k, l_1, l_2 \\ x, y}} (-1)^{L_3+l_{f_2}+l_2+y} \hat{L}_1 \hat{L}_2 \hat{L}_3 \hat{L}^{-1} \hat{x}^2 \hat{y}^2 \\
& \times \begin{Bmatrix} L & y & l_2 \\ l_{f_2} & l_{q_1} & x \end{Bmatrix} \begin{Bmatrix} l_1 & y & l_{f_1} \\ l_{f_2} & L_1 & x \end{Bmatrix} \begin{Bmatrix} L & l_{q_2} & L_3 \\ L_2 & l_{q_1} & x \end{Bmatrix} \begin{Bmatrix} L_1 & L_2 & l_{f_3} \\ l_{q_2} & l_1 & x \end{Bmatrix} \begin{Bmatrix} l_k & l_1 & L \\ y & l_2 & l_{f_1} \end{Bmatrix} \\
& \times [A\mathcal{V}_{kq_1f_1f_2}^{(l_2)} V_{q_2if_3k}^{(l_1)} - C\mathcal{V}_{kq_1f_1f_2}^{(l_2)} W_{q_2if_3k}^{(l_1)} + (-1)^{-S_1} A\mathcal{W}_{kq_1f_1f_2}^{(l_2)} V_{q_2if_3k}^{(l_1)} \\
& + (-1)^{1-S_1} C\mathcal{W}_{kq_1f_1f_2}^{(l_2)} W_{q_2if_3k}^{(l_1)}] E_{kq_1f_1f_2}^{-1}. \tag{A6}
\end{aligned}$$

Spin factors A , B , and C in (A6) are determined by the expressions

$$\begin{aligned}
A &= (-1)^{S_1+S_2+S_3-1/2} \hat{S}_1 \hat{S}_2 \hat{S}_3 \hat{S}^{-1} \begin{Bmatrix} S_1 & \frac{1}{2} & S \\ S_3 & \frac{1}{2} & S_2 \end{Bmatrix} \delta_{SS'} \delta_{M_S M_{S'}}, \\
B &= (-1)^{S_1+S_2-1/2} \hat{S}_2 \hat{S}^{-1} \delta_{S_1 S_3} \delta_{SS'} \delta_{M_S M_{S'}}, \\
C &= (-1)^{S_2-1/2} \hat{S}_1 \hat{S}_2 \hat{S}_3 \hat{S}^{-1} \begin{Bmatrix} \frac{1}{2} & S_3 & S \\ S_2 & S_1 & \frac{1}{2} \end{Bmatrix} \delta_{SS'} \delta_{M_S M_{S'}}. \tag{A7}
\end{aligned}$$

The graphic technique of angular momentum [15,16] is used for the derivation of expression (A6). The summation over n_k in (A6) denotes the summation over the core levels including the discrete excited states and the integration over the continuum spectra.

*Permanent address: A. F. Loffe Physical Technical Institute of the Academy of Science, Leningrad, 194021, Russia.

†Permanent address: Tomsk Polytechnic Institute, Tomsk, 634004, Russia.

- [1] T. A. Carlson and M. O. Krause, *Phys. Rev. Lett.* **14**, 390 (1965).
- [2] U. Becker, D. Szostak, M. Kupsch, H.-G. Kerkhoff, B. Langer, and R. Wehlitz, *J. Phys. B* **22**, 749 (1989).
- [3] N. M. March, W. H. Young, and S. Sampanthar, *The Many-Body Problem in Quantum Mechanics* (Cambridge University Press, Cambridge, 1967).
- [4] I. I. Sobelman, *Atomic Spectra and Radiative Transitions* (Springer-Verlag, Berlin, 1979).
- [5] T. Åberg and G. Howat, in *Encyclopedia of Physics* Vol. 31, edited by S. Flugge and W. Mehlhorn (Springer, Berlin, 1982).
- [6] M. Ya. Amusia, *Atomic Photoeffect* (Plenum, New York, 1990).
- [7] A. B. Migdal and A. J. Krainov, *Approximation Methods in Quantum Mechanics* (Benjamin, New York, 1969).
- [8] L. D. Landau and E. M. Lifshitz, *Quantum Mechanics: Nonrelativistic Theory* (Benjamin, Oxford, 1965).
- [9] T. A. Carlson and M. O. Krause, *Phys. Rev. Lett.* **17**, 1079 (1966).
- [10] A. Ferguson, *Angular Correlation Method in Gamma-Ray Spectroscopy* (North Holland, Amsterdam, 1965).
- [11] N. M. Kabachnik and I. P. Sazhina, *J. Phys. B* **17**, 1335 (1984).
- [12] H. P. Kelly, *Phys. Rev. A* **11**, 556 (1975).
- [13] B. R. Judd, *Second Quantization and Atomic Spectroscopy* (Johns Hopkins University Press, Baltimore, 1967).
- [14] I. Lindgren, and J. Morrison, *Atomic Many-Body Theory* (Springer-Verlag, Berlin, 1985).
- [15] D. A. Varshalovitch, A. N. Moskaliyov, and V. K. Hersonskii, *Quantum Theory of Angular Momentum* (Nauka, Moscow, 1975).
- [16] A. P. Jucys, I. B. Levinson, and V. V. Vanagas, *Mathematical Apparatus of the Theory of Angular Momentum* (Israel Program for Scientific Translations, Jerusalem, 1962).